ELSEVIER

Biochimica et Biophysica Acta 1325 (1997) 250–262

BIOCHIMICA ET BIOPHYSICA ACTA
BBA

# Methyl mercury interactions with phospholipid membranes as reported by fluorescence, $^{31}$P and $^{199}$Hg NMR

Laurent Girault [a,b], Alain Boudou [b], Erick J. Dufourc [a,*]

[a] *Centre de Recherche Paul Pascal, CNRS, Av. A. Schweitzer, 33600 Pessac, France*
[b] *Laboratoire d'Ecotoxicologie, Université Bordeaux I / CNRS, 33405 Talence, France*

Received 2 October 1996; accepted 17 December 1996

**Abstract**

Methylmercury ($CH_3Hg(II)$) interactions with multilamellar vesicles of dimyristoyl(DM)- and dipalmitoyl(DP)-phosphatidylcholine (PC), -phosphatidic acid (PA), -phosphatidylglycerol (PG), -phosphatidylserine (PS) and -phosphatidylethanolamine (PE) have been investigated from the metal viewpoint by solution $^{199}$Hg-NMR and from the membrane side by diphenylhexatriene fluorescence polarization and solid state $^{31}$P-NMR. Results can be summarized as follows: (1) $CH_3Hg(II)$ strong binding to membranes results in a progressive decrease of the free $CH_3HgOH$ $^{199}$Hg-NMR isotropic signal and because of a slow exchange, in the NMR time scale, between free and bound methylmercury pools the lipid/water partition coefficients, $K_{lw}$, of the $CH_3HgOH$ species can be determined in the lamellar gel (fluid) phase. It is found: $K_{lw}(DMPC) \approx 2 \pm 2$ $(2 \pm 2)$; $K_{lw}(DMPE) \approx 7 \pm 3$ $(16 \pm 3)$; $K_{lw}(DMPG) = 170 \pm 10$ $(110 \pm 10)$; $K_{lw}(DMPS) = 930 \pm 50$ $(1250 \pm 60)$; $K_{lw}(DMPA) = 1250 \pm 60$ $(300 \pm 20)$. $CH_3Hg(II)$ interactions with membrane phospholipids are therefore electrostatic in nature and the phosphate moiety is proposed as a potential binding site. (2) The presence of $CH_3HgOH$ stabilizes the PG gel phase and destabilizes that of PS. No effect is observed on PC, PA and PE thermotropism. (3) methylmercury promotes the formation of isotropic $^{31}$P-NMR lines with PG, PA and PE systems suggesting the presence of non-bilayer phases and hence membrane reorganization. The above effects are compared to those of inorganic mercury Hg(II) and discussed in the context of cell toxicity.

*Keywords:* Methyl mercury; Phospholipid membrane; $^{31}$P and $^{199}$Hg nuclear magnetic resonance; Fluorescence; Toxicity

Abbreviations: Hg(II), inorganic mercury; $CH_3Hg(II)$ or MeHg(II), methyl mercury; NMR, nuclear magnetic resonance; PC, phosphatidylcholine; PG, phosphatidylglycerol; PS, phosphatidylserine; PA, phosphatidic acid; PE, phosphatidylethanolamine; PI, phosphatidylinositol; SM, sphingomyelin; DM-PL, dimyristoyl-phospholipid; DP-PL, dipalmitoyl-phospholipid; DPH, diphenylhexatriene; P, fluorescence polarization of DPH; $T_m$, lamellar gel-to-lamellar fluid phase transition temperature; $R_i$, lipid-to-mercury molar ratio; pCl, -log [$Cl^-$]; MLV, multilamellar vesicles; $\delta$, isotropic NMR chemical shift; $\Delta\sigma$, NMR chemical shielding anisotropy; $\Delta\nu_{1/2}$, NMR line-width at half intensity; $K_{ow}$, octanol/water partition coefficient; $K_{lw}$, lipid/water partition coefficient

* Corresponding author. Fax: +33 5 56 845600. E-mail: dufourc@crpp.u-bordeaux.fr


*PII* S0005-2736(96)00263-5

## 1. Introduction

Mercury is a widespread environmental pollutant and methylmercury is considered as the most toxic of all mercury chemical forms. Unfortunately, little is known about the molecular mechanisms controlling its uptake and toxicity. The greater bioaccumulation of $CH_3Hg(II)$ over inorganic mercury Hg(II) is often ascribed to higher lipid solubility of the organic form [1]. However, octanol/water partition coefficients ($K_{ow}$) of uncharged $HgCl_2$ and $CH_3HgCl$ species do not differ significantly (3.3 and 1.7, respectively) [2]. $HgCl_2$ also displays fast diffusion coefficients through lipid bilayers [3,4], and should steadily cross the membrane barrier. Mason et al. [5] indeed showed that diffusion of the Hg(II) and $CH_3Hg(II)$ neutral chloro-complexes controls mercury uptake into unicellular phytoplankton diatom. Nevertheless, methylmercury is the main chemical form accumulated along food webs accounting for up to 95% of total mercury into aquatic carnivorous species, like piscivore fishes [6], and leading to extremely high bioaccumulation factors ($\geq 10^6$). $CH_3Hg(II)$ is also quickly redistributed into the whole body from transfer between donor and acceptor organs [6] and its excretion rates are far lower than those of Hg(II) [7], possibly because inorganic mercury reacts to a larger extent with protective glutathione and metallothioneins [8,9]. As a result, methylmercury is held responsible for most of the mercury toxicity occurring in upper organisms and human populations, as was dramatically proven by the Minamata disease in Japan [10].

Mercury compounds have high affinity for proteic thiol groups [1], but they also induce membrane damage (leakage, rigidification) that probably results from strong interactions with lipids [11,12]. However, only few studies on methylmercury binding to biomembrane lipids have been reported. One must nonetheless mention the work of Segall and Wood [13] who reported that methylmercury catalyses the hydrolysis of vinyl-ether links in plasmalogen PE. Also, Leblanc et al. [14] observed a pH-dependent binding of $CH_3HgCl$ to acidic PS and PI phospholipids, but not to zwitterionic PC and SM.

$^{199}$Hg-NMR has proven to be useful in the study of methylmercury chemical speciation [15] and is applicable to mercury-membrane binding studies [16]. On the other hand, $^{31}$P-NMR of phospholipids and fluorescence polarization have been recently used to probe the consequences of Hg(II) binding on membrane structure and fluidity [17,18]. In this paper, we investigate the interactions between methylmercury and membrane phospholipids using complementary techniques, to probe the effects of $CH_3Hg(II)$ from both the metal and the membrane viewpoints. $^{199}$Hg solution NMR is used to quantify $CH_3HgOH$ binding to multilamellar vesicles (MLV) made of phospholipid dispersions in excess water, whereas $^{31}$P solid state NMR and fluorescence polarization of diphenylhexatriene embedded in the bilayers allow to detect changes in membrane structure and dynamics at the head-group and core levels, respectively. Phospholipids of varied head-groups and acyl chain lengths were employed. The effect of membrane rigidity (gel or fluid phase) on the interactions was also investigated by varying the temperature.

## 2. Materials and methods

### *2.1. Materials*

$CH_3HgOH$ (1 M) in water was obtained from Alfa Inorganics (Karlsruhe, Germany); DMPC, DMPA, DMPS, DMPE, DMPG, DPPS and DPPG were purchased from Avanti Polar Lipids (Alabaster, USA), and DPPA from Bachem (Bubendorf, Switzerland). Morpholino-ethane sulfonic acid (MES) and morpholino-propane sulfonic acid (MOPS) buffers were obtained from Sigma (St. Louis, USA) and diphenylhexatriene (DPH) from Aldrich (Milwaukee, USA). Deionized water was used for buffer preparation. All other compounds were high purity reagents from Prolabo (Paris, France). Possible phospholipid degradation was checked by thin-layer chromatography (TLC) after completion of experiments. No significant hydrolysis was detected.

### *2.2. Sample preparation*

To obtain multilamellar vesicles, phospholipids (50 mM) were dispersed in MES (50 mM, pH = 6.0) by several freeze-thaw-heating cycles and vortex stirring. DMPS was similarly dispersed in MOPS (50 mM, pH 7.0). pH values were chosen so that each anionic phospholipid (i.e., PA, PG, PS) bears only

one negative charge. Note that bilayer structure is not significantly modified by the one-unit pH difference [19]. PE and PC are zwitterionic at both investigated pH. MES and MOPS buffers have similar structure, only differing by one additional -$CH_2$- unit in the MOPS side chain that results in $pK_a$ of 6.0 and 7.0, respectively. We selected these buffers because they do not form complexes with $CH_3Hg(II)$, as shown by preliminary $^{199}$Hg-NMR experiments (see Section 3). To form (1:1) DMPA/DMPC MLV, DMPA and DMPC were first mixed together in $CHCl_3$ and stirred, then the solvent was evaporated under gentle $N_2$ flow and the phospholipids dispersed in MES as described above.

For NMR experiments, variable amounts of MLV solutions (0–500 $\mu$l) were added to 75 $\mu$l $CH_3HgOH$ from a stock solution (1 M), then samples were completed to 1.5 ml with appropriate buffer and stirred ($[CH_3HgOH] = 50$ mM, $R_i =$ [lipid]/[$CH_3HgOH$] ranging from 0 to 1.2). An external mercury reference (sealed glass tube, see NMR data) was added to samples for $^{199}$Hg-NMR only. Sample pH was checked before NMR acquisition and after 8 h delay.

Assuming that hydroxide ions and buffers are the only $CH_3Hg(II)$ ligands to be considered in solution, chemical speciation models based on available thermodynamic data [15] predict that $CH_3HgOH$ soluble species accounts for at least 95% of total $CH_3Hg(II)$ in our experimental conditions (pH = 6.0 to 7.0). The remaining 5% correspond to the $(CH_3Hg)_2OH^+$ bimolecular species. Dissociated ionic $CH_3Hg(H_2O)^+$ represents less than 0.1% of total $CH_3Hg(II)$ in solution.

### 2.3. Fluorescence polarization

Stock solutions of phospholipid MLV were prepared in adequate buffer by vortexing the lipid (6 mM) and the fluorescent probe DPH (1% vol. from a stock solution of 6 mM in tetrahydrofuran), to a final DPH/lipid molar ratio of 0.01. Aliquots were diluted in buffer ([PL] = 0.2 mM) and enclosed in 10-mm wide quartz cells; DPH fluorescence polarization (P) was measured as previously described [17], as a function of temperature ($\pm$0.1°C), in the absence and presence of $CH_3HgOH$ ($R_i = 1$). Sample cooling was operated manually and cooling rate was about 10°C/h. In $^{31}$P-NMR experiments we observed that sample equilibration is fast (less than 1 h) except for $CH_3Hg(II)$-PE systems that evolve for 3–4 h before stabilization (see Section 3); so a 4-h delay between methylmercury addition and data acquisition was kept with all samples. Each data point was the average of three separate measurements. We have previously checked by spectrofluorimetry performed on a SLM 8000 spectrometer that DPH steady-state fluorescence is unaffected by methylmercury (data not shown).

### 2.4. NMR

$^{199}$Hg-NMR and $^{31}$P-NMR spectra were recorded using 10 mm diameter NMR tubes on a Bruker ARX 300 spectrometer operating in unlocked mode. $^{31}$P-NMR was performed at 121.5 MHz with the Hahn-echo sequence [20] under $^1$H spin-lock decoupling conditions [21], using a 50 kHz spectral window, 2800 scans, 9 $\mu$s $\pi/2$ pulses, 6 s recycle time and a 30 $\mu$s delay between the pulses to form the echo. A Lorentzian line broadening of 100 Hz was applied before Fourier transformation. $^{31}$P-NMR chemical shifts are given relative to 85% $H_3PO_4$, and chemical shift anisotropies ($\Delta\sigma$) are measured with a 1–3 ppm accuracy. $^{199}$Hg-NMR spectra were acquired at 53.7 MHz using the single pulse acquisition sequence with gated broadband proton decoupling, in the presence of a sealed external reference ($HgCl_2$ [1 M] in ethanol, Ø = 3 mm, vol. 100 $\mu$L, $\delta = -1207$ ppm) for calibration. A $T_1$ value of 1.7 s was determined for $CH_3HgOH$ 0.1 M in water using an impulsion-recovery sequence. Typical experimental parameters were: 50 kHz window, 400 scans, 13 $\mu$s $\pi/2$ pulses and 10 s recycle time. $^{199}$Hg-NMR chemical shifts are relative to neat dimethylmercury. Peak area integration was performed using Bruker standard software. Reference peak area was used to calculate sample mole number and concentration, with 10% accuracy.

In order to explore the consequences of the membrane physical state (gel or fluid) on lipid-methylmercury interactions, NMR experiments were performed at two temperatures: 24°C and at a temperature 5°C above the main transition temperature of the $CH_3Hg(II)$-lipid system, as determined by fluorescence polarization. Dimyristoyl-phospholipids em-

ployed in this study are either in the gel phase (DMPA, DMPE, DMPS, DMPG) or close to the gel-to-fluid phase transition (DMPC) at 24°C, so that except for DMPC, the two temperatures are representative of systems in their lamellar gel and fluid phases.

## 3. Results

### 3.1. Fluorescence polarization

Fluorescence polarization of DPH embedded in phospholipid MLV as a function of temperature, in the absence and presence of $CH_3HgOH$ ($R_i = 1$), is shown on Fig. 1. The polarisation (P) of DPH embedded in a lipid bilayer is related to the membrane physical state: *P*-values are high in the gel-crystalline phase and low in the fluid phase [22]. Thermotropic variations therefore allow determination of the fluid-to-gel phase transition temperature ($T_m$) of the system, depending on its composition and on the presence of $CH_3HgOH$. Methylmercury addition has no significant effect on *P*-values in the gel and fluid phases of the different MLV studied. Only a slight increase of *P* in DMPE bilayers in the gel phase is observed in the presence of methylmercury.

Main phase transition temperatures $T_m$ as estimated from DPH fluorescence polarization curves are reported in Table 1. They are in good agreement with already published data [23]. Methylmercury induces a significant decrease of the $T_m$ value of PS vesicles that depends on the lipid chain length (DMPS: −6.3°C; DPPS: −2.9°C). In contrast, $CH_3HgOH$ causes an increase of the $T_m$ value of DMPG and DPPG vesicles (+3.6°C and +6.5°C, respectively). No significant $T_m$ changes are detected for DMPC, DMPA and DPPA.

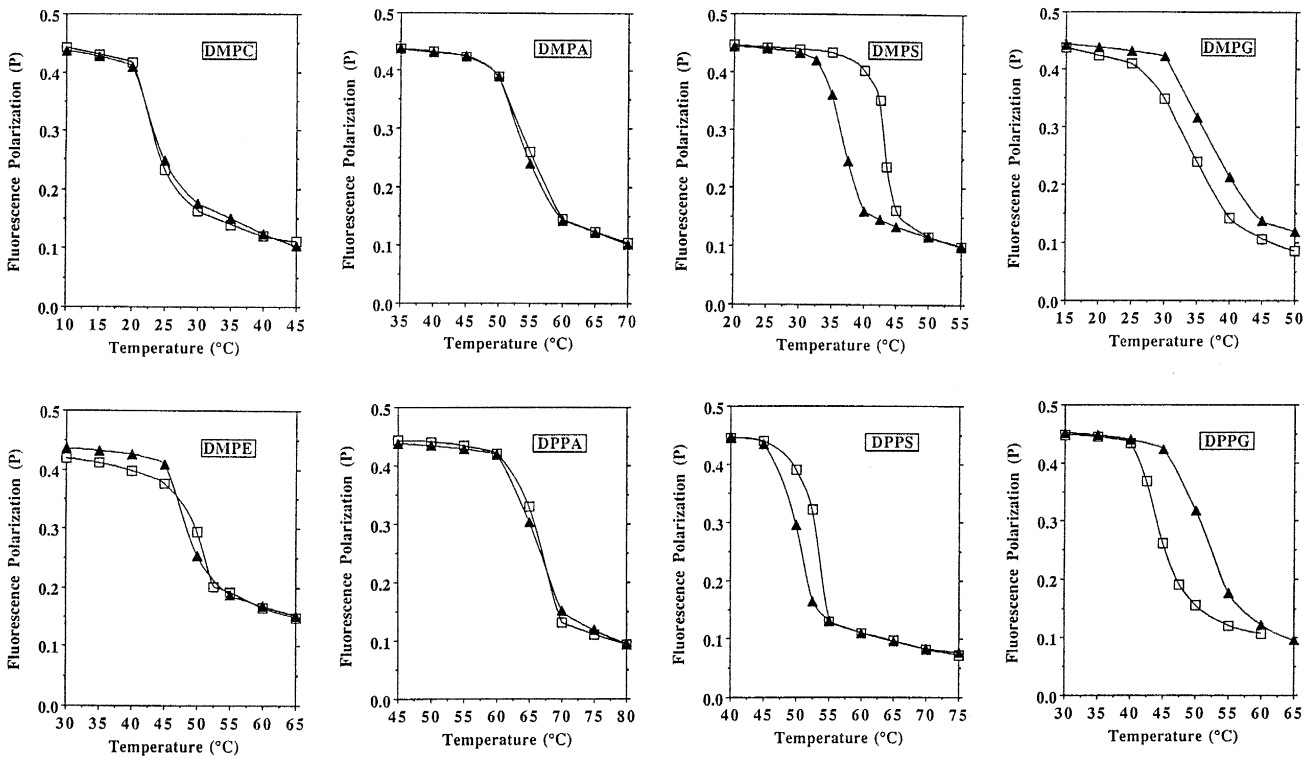


Fig. 1. Fluorescence polarization (P) of DPH (60 μM) embedded in multilamellar vesicles of phospholipids (6 mM in MES or MOPS buffers, pH 6 or 7) as a function of temperature, in the absence (□) and presence (▲) of $CH_3HgOH$ ($R_i = 1$). Nature of phospholipid is indicated on graph. Solid lines are drawn to help reading the figures. $\lambda_{emission} = 360$ nm, $\lambda_{detection} = 445$ nm.

Table 1
Main phase transition temperatures ($T_m$) of phospholipid multilamellar vesicles

| | DMPC | DMPE | DMPA | DPPA | DMPS | DPPS | DMPG | DPPG |
|---|---|---|---|---|---|---|---|---|
| Pure systems | 23.5 | 50.2 | 55.0 | 66.8 | 43.6 | 53.1 | 33.8 | 44.2 |
| $+CH_3Hg(II)$ | 23.3 | 49.0 | 54.6 | 66.4 | 37.3 | 50.2 | 37.4 | 50.7 |
| $\Delta T_m$ | −0.2 | −1.2 | −0.4 | −0.4 | −6.3 | −2.9 | +3.6 | +6.5 |

$T_m$ values are given in Celsius degrees, with a 0.6°C accuracy. They are estimated from the fluorescence polarization measurements of 60 $\mu$M DPH embedded in 6 mM MLV, in the absence and presence of $CH_3HgOH$ ($R_i = 1$).

### 3.2. $^{31}$P-NMR

$^{31}$P-NMR powder spectra of MLV in the absence and presence of $CH_3HgOH$ ($R_i = 1$) are given in Fig. 2. Spectra for controls at 24°C show well-defined, axially symmetric line-shapes characteristic of the lamellar fluid (DMPC) or gel phases (DMPE, DMPA, DMPG, DMPS) (Fig. 2a). Controls at $T_m$ +5°C ($T_m$ defined from Fig. 1) all show spectral shapes characteristic of the lamellar fluid phase (Fig. 2b). However, DMPA and DMPS spectra show some percent of an isotropic component, which can be interpreted

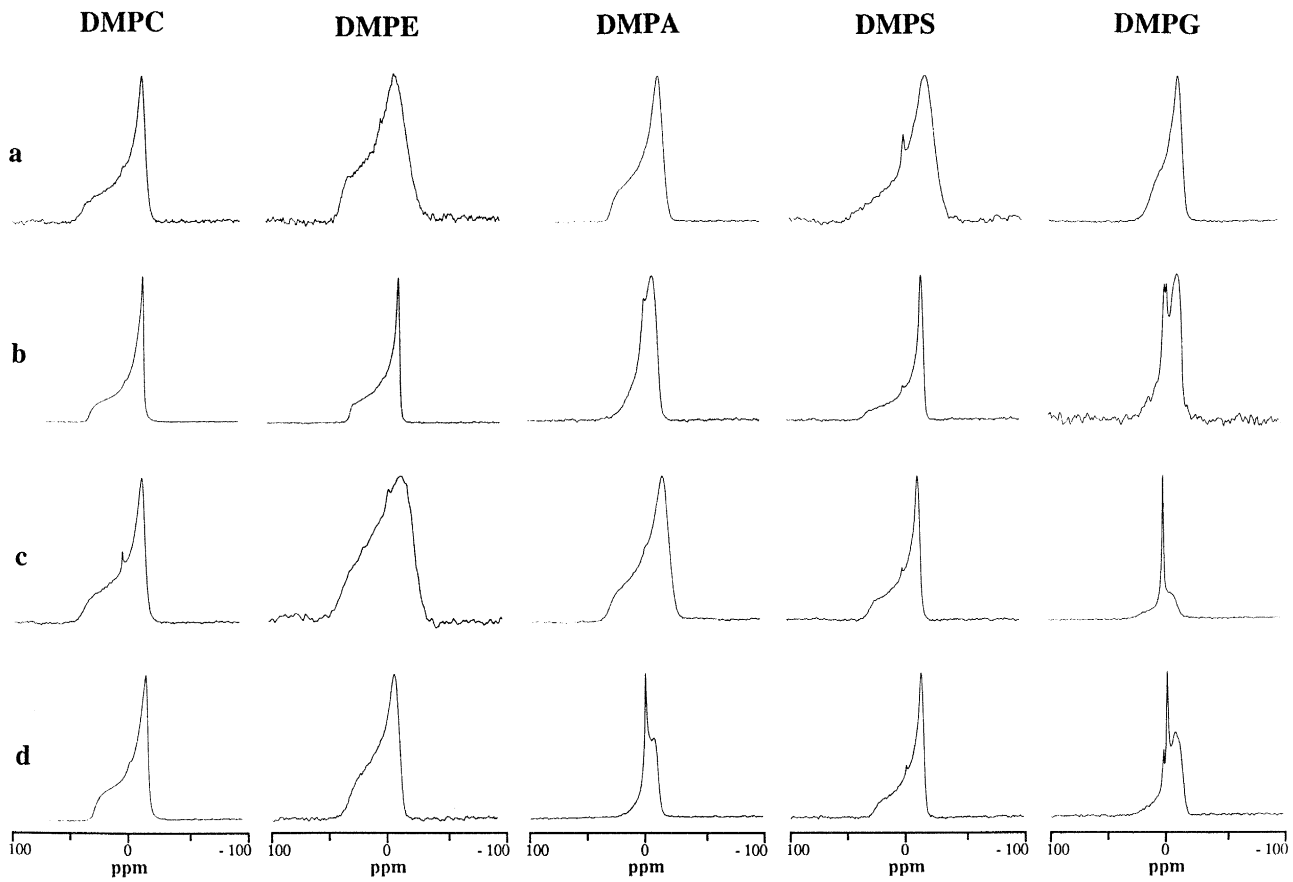


Fig. 2. $^{31}$P-NMR spectra of phospholipid multilamellar vesicles, in the absence and presence of $CH_3HgOH$ ($R_i = 1$). Top spectra are controls: (a) $T = 24$°C, (b) +5°C over $T_m$ of the mercury-lipid systems, i.e., 35°C for DMPC, 50°C for DMPE, DMPG, DMPS and 65°C for DMPA. Bottom spectra were acquired after $CH_3HgOH$ addition and equilibration: (c) $T = 24$°C, (d) +5°C over $T_m$. Chemical shifts are expressed relative to 85% $H_3PO_4$.

Table 2
$^{31}$P-NMR chemical shift anisotropy ($\Delta\sigma$) values of phospholipid multilamellar vesicles

| | DMPC | DMPE | DMPA | DMPS | DMPG |
|---|---|---|---|---|---|
| Pure systems (gel phase) | 49 | 46 | 40 | 55 | 31 |
| Pure systems (fluid phase) | 42 | 40 | 28 | 46 | 30 |
| + $CH_3Hg(II)$ (gel phase) | 47 | 52 **(+6)** | 46 **(+6)** | 38 **(− 17)** | 30 |
| + $CH_3Hg(II)$ (fluid phase) | 42 | 41 | 28 | 38 **(− 8)** | 30 |

Chemical shift anisotropy values are measured in ppm, with a 3 ppm accuracy. $CH_3HgOH$ was added at $R_i = 1$. Gel phase temperature is 24°C for all lipids, except for DMPC whose $T_m$ is about 24°C. Fluid phase temperatures (above $T_m$) are 35°C for DMPC, 50°C for DMPE, DMPG, DMPS and 65°C for DMPA. Significant chemical shift anisotropy changes induced by $CH_3HgOH$ are noted in bold.

as a formation of micelles or small unilamellar vesicles [24]. The same is observed with DMPG, but another minor spectral component appears, possibly related to hexagonal $H_{II}$ phase formation [25].

With the exception of DMPE, methylmercury-induced line-shape changes occur within 1 h following methylmercury addition, and $^{31}$P-NMR spectra are stable thereafter. Isotropic line accounts for more than 50% of the DMPG spectra in the presence of methylmercury, revealing an extensive lipid phase restructuration (Fig. 2c). $CH_3HgOH$ addition to DMPE MLV induces a slow change of the $^{31}$P-NMR spectra, leading in 4 h to the rise of a new, broad spectrum, while the initial gel phase spectrum progressively disappear. Transient formation of an intense isotropic line is observed (data not shown). $CH_3Hg(II)$-DMPE samples immediately lay down in the NMR tubes, forming a solid precipitate. Upon increasing temperature above the lipid-methylmercury $T_m$ (Fig. 2d), temperature-induced isotropic line formation with DMPA and DMPG vesicles is enhanced in the presence of $CH_3HgOH$. However, mercury-induced isotropic line is less intense at 50°C than at 24°C for DMPG. The $CH_3Hg(II)$-DMPE spectral line-shape is still very broad compared to the control.

Chemical shift anisotropies ($\Delta\sigma$) were measured between the low-field shoulder and the high-field peak and reported in Table 2. $\Delta\sigma$ values are typically lower for lipids in fluid phase than in gel phase. Upon $CH_3HgOH$ addition at $T = 24$°C, one observes a significant $\Delta\sigma$ increase for DMPA and DMPE MLV spectra while $\Delta\sigma$ is reduced for DMPS and unaffected for DMPG and DMPC. Methylmercury-induced $\Delta\sigma$ increase disappears in the fluid phase: values are then similar to controls for DMPE and DMPA. The very large $\Delta\sigma$ decrease observed at 24°C with DMPS is only halved at 50°C.

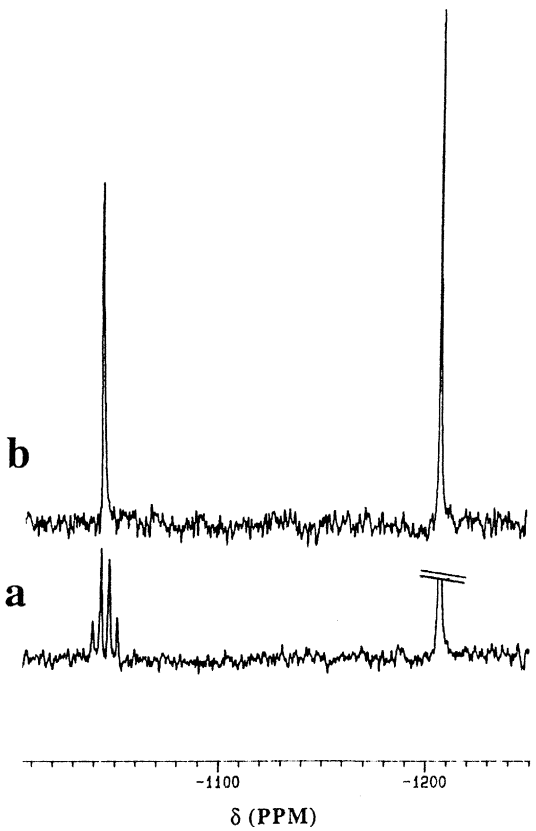


Fig. 3. $^{199}$Hg-NMR spectra of 50 mM $CH_3HgOH$ in MES buffer (50 mM, pH 6.0, $T = 24$°C): (a) without $^1$H decoupling, and (b) under $^1$H-broad-band decoupling conditions. Right NMR signal corresponds to an external reference ($HgCl_2$ [1M] in ethanol, $\delta = -1207$ ppm). Chemical shifts are expressed relative to neat dimethylmercury.

### 3.3. Hg-NMR

Fig. 3 shows the $^{199}$Hg-NMR spectra of 50 mM $CH_3HgOH$ in MES buffer (pH 6.0) at 24°C. Right signal corresponds to the $HgCl_2$ external reference. $^{199}$Hg coupling with the three equivalent protons of the methyl group results in a quadruplet spectrum for $CH_3HgOH$ (left), with intensities (1:3:3:1) (Fig. 3a). The measured ($^1$H-$^{199}$Hg) $^2J$ coupling constant is 210 Hz. Under $^1$H broadband decoupling conditions, a single isotropic line is observed instead (Fig. 3b). Increasing concentrations of MES and MOPS (up to 0.25 M, at constant pH) induced no change on spectra 3b, while addition of Tris or Hepes buffers caused significant chemical shift changes of the $CH_3Hg(II)$ isotropic line, indicating the formation of soluble $CH_3Hg(II)$-buffer species (data not shown). We therefore conclude that MES and MOPS do not form complexes with aqueous methylmercury in our experimental conditions: they do not modify the free metal ion concentration and are therefore adequate for $CH_3Hg(II)$ speciation studies, unlike Tris or Hepes. To corroborate with available thermodynamic data, the $^{199}$Hg-NMR chemical shift of 50 mM $CH_3Hg(II)$ was also recorded as a function of pH in water, yielding a standard pH-titration curve with $pK_a = 4.85 \pm 0.10$ (data not shown). The minor discrepancy compared to the $pK_a = 4.67$ found in the literature [15] may be attributed to $(CH_3Hg)_2OH^+$ formation.

$CH_3HgOH$ (50 mM) was added to phospholipids multilamellar vesicles ($R_i$ from 0 to 1.2), both at 24°C and above the mercury-lipid systems $T_m$. Two general observations can be drawn: (1) The $CH_3Hg(II)$ isotropic line chemical shift ($\delta_{obs}$) remained constant during all experiments conducted in the presence of phospholipids, for a given set of pH and temperature conditions (data not shown). (2) In all cases, the $^{199}$Hg-NMR isotropic signal progressively disappears upon MLV addition, except with DMPC (Fig. 4). Negatively charged phospholipids

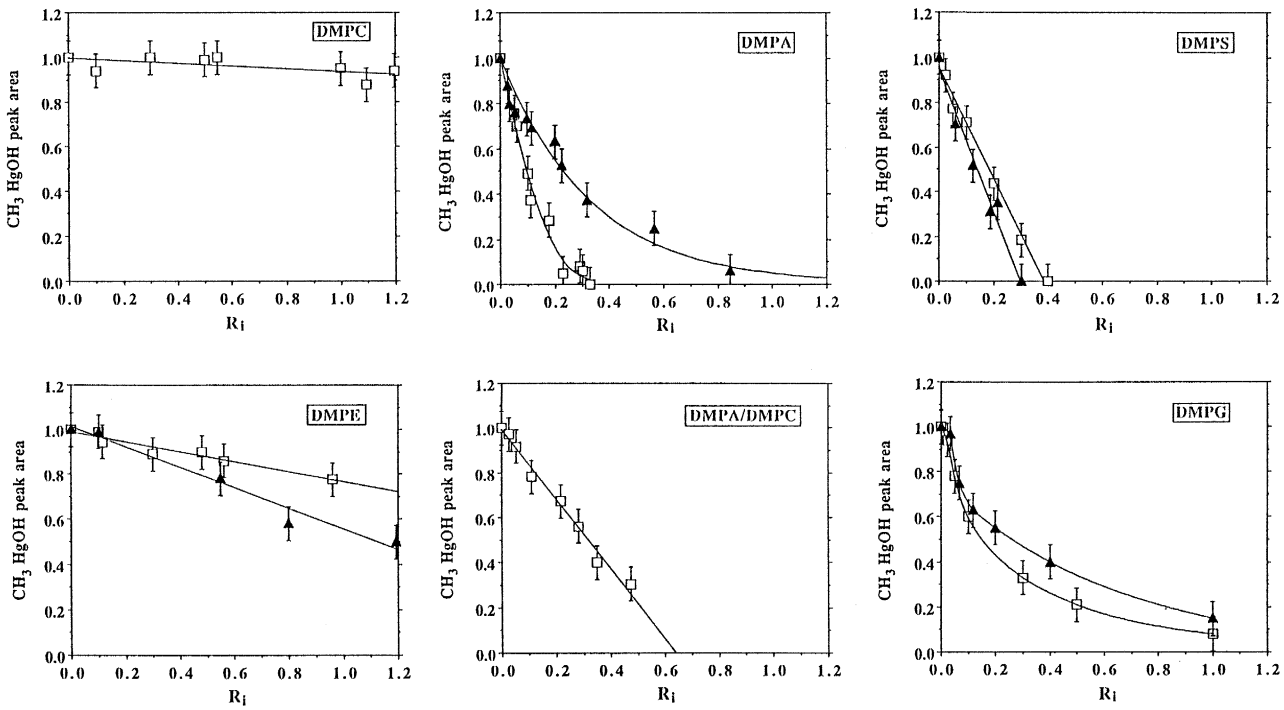


Fig. 4. $^{199}$Hg-NMR peak area decrease of 50 mM $CH_3HgOH$, as a function of lipid-to-metal molar ratio ($R_i$). Control area is 1 at $R_i = 0$. Nature of added phospholipid is indicated on graphs. $CH_3HgOH$ peak area decrease was measured by comparing with the external reference constant peak area. Temperature is 24°C (□) or +5°C above the $T_m$ of the lipid-mercury system (▲), as determined by DPH fluorescence polarization, i.e., 50°C for DMPE, DMPG, DMPS and 65°C for DMPA. DMPC data are unaffected by temperature hence only the 24°C curve is shown for clarity. Data points are the means of 2–4 independent measurements, giving a ±5% accuracy on peak areas. Solid lines are drawn to help reading the figures.

(DMPA, DMPS and DMPG) induce sharp peak area decreases: at 24°C, addition of DMPA or DMPS results in complete loss of signal at $R_i = 0.3$ and 0.4, respectively, while a plateau tendency is observed with DMPG. The peak area at the plateau value corresponds to $CH_3HgOH$ remaining in solution, about 10% at $R_i = 1$. DMPE is much less effective, reducing the peak area by only 25% at $R_i = 1$. Peak area is not significantly affected by DMPC addition, up to $R_i = 1.2$. Mixed DMPA/DMPC (1:1) MLV show intermediate effect on $CH_3HgOH$ signal when compared to DMPA or DMPC. NMR peak areas vary linearly (DMPS, DMPE, DMPA/DMPC 1:1) or exponentially (DMPA, DMPG) with $R_i$.

Increasing the temperature above the $T_m$ of the lipid-mercury systems markedly reduces the effect of DMPA on $CH_3HgOH$ peak area. One must mention that a broad component (line-width of ca. 2000 Hz and chemical shift very close to that of the sharp line) is observed in addition to the isotropic signal (data not shown). This additional component is only detected in the presence of DMPA and may be reminiscent of a slow-to-intermediate exchange regime of a fraction of mercury in solution with this membrane (vide infra). This signal was taken into account for peak area calculation. Moving to the fluid phase also reduces the effect of DMPG addition by increasing the plateau value to 17% at $R_i = 1$, though no significant changes are observed below $R_i = 0.1$. DMPS-induced peak area decrease is enhanced in the fluid phase, resulting in a loss of detectable signal at $R_i = 0.3$, instead of 0.4 at 24°C. DMPE effect is also approximately doubled above $T_m$ while increasing temperature does not change the DMPC binding curve (data not shown). Spectra of $CH_3HgOH$ in the presence of DMPA or DMPG ($R_i = 0.1$) were taken at various temperatures above the mercury-lipid $T_m$. In these conditions, i.e., within a given membrane physical phase, temperature has no significant effect on peak area decrease. Previously observed changes are therefore attributable to the gel-to-fluid phase transition. As a whole, the effect of phospholipids that yield a linear binding curve is increased on going from the gel to the fluid phase, while it is reduced for those with an exponential binding curve.

A progressive broadening of $^{199}$Hg-NMR $CH_3HgOH$ signals is observed upon MLV addition, the effect being dependent on $R_i$, temperature and the lipid head-group (data not shown). Line-width ($\Delta\nu_{1/2}$) were also measured at half-signal intensity. Phospholipid effects on both peak area and line-width of $CH_3HgOH$ signal display the same head-group specificity: PA > PS > PG ≫ PE > PC. Temperature increase results in additional signal broadening, but the specificity order indicated above is conserved. $\Delta\nu_{1/2}$ values increase linearly with $R_i$ for acidic phospholipids, from 50 Hz for controls to 300–600 Hz at high $R_i$. Only a slight ($\times 2$) signal broadening is observed with both DMPC and DMPE.

Slight increase of samples pH are observed when significant $CH_3Hg(II)$ peak area decrease takes place. The pH increase depends on the amount of peak area decrease ($+0.15$ for 50% peak reduction, $+0.3$ for 100% decrease), but not on the nature of the phospholipid head-groups.

## 4. Discussion

In this work the interaction of methylmercury with phospholipid membranes has been monitored from both the metal and the membrane viewpoints using three complementary techniques: (a) $^{199}$Hg-NMR which quantitatively describes $CH_3Hg(II)$ mobility and complexation, both in solution and at the membrane interface, without perturbing the thermodynamic equilibrium conditions [16], (b) fluorescence polarization which reveals dynamical changes of the bilayer hydrophobic interior [22] and (c) solid state $^{31}$P-NMR which is indicative of the phosphate group structure and mobility and allows detection of non-bilayer phases [18]. An overall vision of membrane fluidity and integrity changes occurring upon methylmercury complexation can therefore be obtained, enabling us to relate the observed macroscopic effects to specific molecular mechanisms.

To summarize, we have shown that $CH_3Hg(II)$ complexation primarily depends on the polar head groups negative charges and to a lesser extent on the membrane physical state. Extensive metal binding (up to three $CH_3Hg(II)$ molecules per lipid) induces limited perturbations of the lamellar phase thermotropism with, however, in some cases loss of its integrity. These different aspects are discussed below and a comparison with the already reported effects of inorganic Hg(II) on phospholipid membranes [18] is

made. The nature of methylmercury interaction mechanisms with phospholipids are also discussed, in relation with the $CH_3Hg(II)$ chemical speciation.

### *4.1. Methylmercury binding*

Three readily observable experimental parameters on the $^{199}$Hg-NMR spectra of $CH_3Hg(II)$ can report on the metal complexation with ligands: (1) the observed isotropic line chemical shift ($\delta_{obs}$) is highly sensitive to methylmercury complexation in the aqueous phase and to exchange with bound species [16]. When ligands exchange is fast in the NMR time scale (exchange rate $\gg 10^3$ Hz), $\delta_{obs}$ is the pondered mean of the individual chemical species $\delta$ values. Therefore, the slightest change in speciation of mercury soluble species results in chemical shift changes of several ppm [15,26]. (2) the $^{199}$Hg-NMR chemical shift anisotropy in solids may be of several MHz [27] which implies that signal of methylmercury bound to an extended lipid lamellar phase is therefore broadened beyond detection by solution NMR. This results in apparent peak area decrease of the signal in solution and allows quantitative determination of bound methylmercury. In these conditions, 'bound' and 'free' mercury pools are in slow exchange in the solid state NMR time scale (exchange rate $< 10^6$ Hz), evidencing formation of stable complexes of $CH_3Hg(II)$ with phospholipid head-groups, with long lifetimes. (3) Finally, line broadening of NMR signals in solution may be indicative of restricted mobility of the observed nucleus or may arise from intermediate exchange regime between the observed signals.

In our experiments, $\delta_{obs}$ values are only affected by pH and temperature and are remarkably constant in the presence of phospholipids at any $R_i$, indicating that $CH_3HgOH$ remains uncomplexed in the bulk solution. Kinetics of methylmercury binding to the phospholipid bilayers are directly proportional to the initial rates of peak area decrease measured at low molar ratio on Fig. 4. At 24°C, i.e., in or near the gel phase, DMPC < DMPG ≈ DMPA, whereas in the fluid phase they rank as DMPC < DMPS ≈ DMPG. On going through the gel-to-fluid phase transition, methylmercury binding to DMPA and DMPG decreases (Fig. 4). Therefore, increased membrane fluidity frees $CH_3Hg(II)$ interactions with PA and PG. At converse, PS and PE bilayers bind more $CH_3Hg(II)$ in the fluid phase. Such a phase dependence of PE and PS binding could result from deeper $CH_3Hg(II)$ inclusion in the bilayers, i.e., close to the beginning of the acyl chains. Boudou et al. [28] indeed observed the quenching by methylmercury of the pyrene fluorescent probe imbedded in the central core of PS membranes.

Metal partitioning into a membrane can be defined by the bound-to-free metal ratio. Lakowicz and Anderson [29] calculated such a lipid/water partition coefficient, $K_{lw}$, for $CH_3HgCl$ in DMPC vesicles. Assuming that 100 mM phospholipids in water occupied about 10% of total sample volume they found $K_{lw} \leq 2$. On the same basis we can calculate $K_{lw}$ values for $CH_3HgOH$-DMPL systems:

$$K_{lw}(\text{DMPL}) = (\text{water vol.}/\text{lipid vol.}) \times \left([CH_3Hg(II)]_{bound}/[CH_3Hg(II)]_{free}\right)$$

Bound-to-free molar ratio is estimated from the $CH_3HgOH$ peak area at saturation or peak disappearance depending on the shape of curves in Fig. 4 (accuracy of ±5%). It must be mentioned that in the case of DMPC and DMPE only rough estimates can be given because the $^{199}$Hg-NMR line never disappears nor gets saturated in our range of $R_i$. This leads to the following results: at 24°C, $K_{lw}(\text{DMPC}) \approx 2 \pm 2$; $K_{lw}(\text{DMPE}) \approx 7 \pm 3$; $K_{lw}(\text{DMPG}) = 170 \pm 10$; $K_{lw}(\text{DMPS}) = 930 \pm 50$; $K_{lw}(\text{DMPA}) = 1250 \pm 60$. In the fluid phase, one obtains: $K_{lw}(\text{DMPC}) \approx 2 \pm 2$; $K_{lw}(\text{DMPE}) \approx 16 \pm 3$; $K_{lw}(\text{DMPG}) = 110 \pm 10$; $K_{lw}(\text{DMPA}) = 300 \pm 20$; $K_{lw}(\text{DMPS}) = 1250 \pm 60$. Interestingly, this affinity order is not exactly the same as that obtained by measuring initial rates of binding. This is related to the fact that the PA and PG binding curves are exponential, whereas those of PS are linear. It is nonetheless clear that binding is greater by at least two orders of magnitude with anionic lipids than with zwitterionic.

The progressive broadening of free methylmercury isotropic signal with increasing phospholipid concentrations could indicate near-intermediate exchange rates with bound metal, instead of really slow ones. However, given the sensitivity of the $^{199}$Hg-NMR chemical shift to ligands, some significant $\delta_{obs}$ should be simultaneously observed. Alternatively, signal

broadening could result of a reduced mobility of the soluble $CH_3HgOH$ species. It is possible that 'free' $CH_3HgOH$ actually diffuses through lipid bilayers without interacting strongly with specific sites, while 'bound' metal is more permanently fixed onto such sites. This would be in agreement with studies demonstrating slowed diffusion rates of $CH_3HgCl$ in the presence of PC vesicles [29]. Head-group specificity as far as isotropic line broadening is concerned is about the same as that observed for $CH_3Hg(II)$ binding. The $R_i$-dependant pH increase observed upon MLV addition can be attributed to $CH_3HgOH$ dissociation, yielding $CH_3Hg^+$ and $OH^-$. $CH_3Hg(H_2O)^+$ therefore should be the mercury reactive species, confirming the basically electrostatic nature of $CH_3Hg(II)$-phospholipid interactions.

As already mentioned $CH_3HgCl$ partitions in octanol preferentially to $CH_3HgOH$ ($K_{ow} = 1.7$ compared to 0.07) [2]. Stary and Kratzer [38] and Mason et al. [5] observed an increase of methylmercury uptake into unicellular algae with high chloride concentrations, both in vivo and in vitro. They explained this result by assuming that $CH_3HgCl$ diffusion was the main process of methylmercury bioaccumulation in algae. However, it was previously noted that $CH_3Hg(II)$ accessibility to the core of model membranes was strongly dependent on the membrane charge and that $CH_3HgOH$ was twice more efficient than $CH_3HgCl$ to quench a core-imbedded probe, though both species showed increased efficiency upon increasing the membrane negative charge [28]. Our results explain and support these observations. From the $K_{lw}$ values calculated herein and that reported by Lakowicz and Anderson [29], it is obvious that $CH_3HgOH$ accumulates in negative lipidic membranes to a much greater extent ($\times 600$) than does $CH_3HgCl$, both in lipid and in octanol media. However, one must keep in mind that biological membranes are three-layers barriers (hydrophilic-hydrophobic-hydrophilic), while octanol-water systems are interfacial monolayers that only mimic the central, hydrophobic compartment of a membrane. Consequently, the use of $K_{ow}$ values to predict the ability of a molecule to cross biomembranes seems insufficient, at best. Depending on membrane charge and composition, electrostatic attraction and binding of cationic $CH_3Hg^+$, followed by translocation of the neutralized lipid-mercury species across the bilayer, could display kinetics much faster than the rate of $CH_3HgCl$ free diffusion from the bulk solution. This 'facilitated diffusion' mechanism has indeed been shown to control the uptake through biomembranes of other cationic organometals like tributylin [39]. Unfortunately, we were not able to obtain $^{199}$Hg-NMR spectra of $CH_3HgCl$ with a satisfactory signal-to-noise ratio, due to low solubility and possibly to relaxation factors. This postpones the discussion about the relative efficiencies of $CH_3HgCl$ versus $CH_3HgOH$.

### *4.2. Consequences of methylmercury binding on membrane structure*

Methylmercury shows relatively weak effects on the lipid phase transition temperatures (Table 1). This is easily understandable since, as a monovalent cation, $CH_3Hg(II)$ is expected to give (1:1) complexes with phospholipids and cannot bind several head-groups together to form rigid gel or cochleate phases. On the other hand, divalent cations like $Ca^{2+}$ are able to bridge several head-groups, inducing large shifts of the $T_m$ value of negatively charged phospholipids. The dehydrated $Ca(PS)_2$ cochleate, for example, has a $T_m$ of 155°C [30]. Given the high head-group-specificity of $CH_3Hg(II)$-induced $T_m$ shifts, these are probably consequences, felt at the chains level, of slight changes in the interactions between adjacent head-groups. Binding to serine results in PS membranes destabilization and a $T_m$ decrease: the effect is stronger on short chains lipids (DMPS) than on DPPS, possibly due to greater relative influence of chain length over head-group in overall membrane cohesion. $CH_3Hg(II)$ increases the stability of PG gel phases, either by forming new hydrogen bridges between phosphate groups, or by increasing the packing of the glycerol heads. Stabilization effects increase with chain length, favoring the latter, steric hypothesis. The $T_m$ of PA membranes is unaffected by methylmercury, suggesting that $CH_3Hg(II)$ binding to the phosphate group is a surface reaction that does not sterically perturb the packing of acyl chains. This agrees well with the recent finding that chain dynamics of PA lipids are not correlated with the charge distribution borne by the phosphate head group [40].

Greater methylmercury effects on head-groups are

detected by $^{31}$P-NMR, compared to the chains level, which is coherent with $CH_3Hg(II)$ binding mostly at the membrane surface. The $\Delta\sigma$ variations observed at 24°C reveal changes either in the phosphorus motions or in the head-group tilt angle relative to the bilayer normal [31,32]. Methylmercury complexation with DMPS induces a decrease in the main phase transition temperature, as shown by fluorescence polarization, together with strong $\Delta\sigma$ decrease. Thus, it appears that $CH_3Hg(II)$ could disrupt inter-head-group interactions (electrostatic pairing or hydrogen bonding) that otherwise restrict the movements of the phospholipid molecule. Similar results have been reported for lanthanide interaction with DMPS small liposomes [24]. Conversely, methylmercury binding to PG results in a $T_m$ increase in fluorescence polarization. Lack of $^{31}$P-NMR $\Delta\sigma$ variation is consistent with an increased packing of the phospholipid molecules, without marked changes in the phosphate group movements. On the other hand, the $\Delta\sigma$ increase observed with DMPA and DMPE certainly results from a steric hindrance caused by direct phosphate-$CH_3Hg(II)$ binding. The increase of DMPE spectrum line-width reflects a decrease of the lipid motions that are slow in the NMR time scale (collective motions and lateral diffusion [21]). Above $T_m$, the mercury-induced changes on $\Delta\sigma$ disappear or are markedly reduced, possibly because increased phospholipid mobility suppresses contact between adjacent head-groups and related $CH_3Hg(II)$ steric effects. However, the DMPE-$CH_3Hg(II)$ spectrum remains broader than controls, again suggesting slowed membrane collective motions even when chains are in the fluid phase.

$^{31}$P-NMR isotropic lines are observed upon methylmercury addition to DMPE, DMPG, and to DMPA in the fluid phase (only). Isotropic lines may account for the presence of micelles or small vesicles ($Ø < 500$ Å), with rotational correlation times less than the nanosecond, and might reveal membrane destructuration in the presence of methylmercury. Isotropic line formation increases at high temperatures, possibly as a consequence of increased molecular motions in the fluid phase, i.e., a greater increase in chain volume relative to that of the head group. The absence of temperature-driven increase of the latter would then be linked to a tight MeHg(II) binding at the head group level.

### *4.3. Comparative effects of Hg(II) and $CH_3Hg(II)$ on phospholipid bilayers*

$HgCl_2$ binding to phospholipids MLV has been studied by Delnomdedieu et al. [16,17] using $^{199}$Hg-NMR and DPH fluorescence polarization. Large $^{199}$Hg-NMR chemical shift changes revealed the presence of a labile Hg(II)-phospholipid species in fast or intermediate exchange (in the NMR time scale) with bulk $HgCl_2$. However, the most striking variance with our study is the completely different head-group specificity of $HgCl_2$ compared to $CH_3HgOH$. $HgCl_2$ displayed strong affinity for the primary amine groups of PE and PS, independently of the polar head electric charges and had little or no affinity to negatively charged PA or PG. Fluorescence polarization and $^{31}$P-NMR revealed formation of a rigid, gel-like phase of Hg(II) with PE and PS bilayers that completely abolished the gel-to-fluid and fluid-to-hexagonal phase transitions [17,18]. These effects were highly specific of the neutral $HgCl_2$ species and could be reversed by chloride addition, that resulted in $HgCl_4^{2-}$ formation [16].

Differences between $HgCl_2$ and $CH_3HgOH$ specificities towards phospholipids can be accounted for by making use of thermodynamic considerations. Neutral $HgCl_2$ is very stable, with a cumulative formation constant $\beta_2 = 10^{13.1}$ and can only dissociate to bind ligands of equal or stronger affinity (at similar ligand concentrations), such as phospholipid amines (calculated $\beta_1 = 10^{12.7}$ for Hg(PE) and $\beta_2 = 10^{13.3}$ for $Hg(PS)_2$ [16]). $CH_3Hg(II)$ affinities to counterions are lower ( $\beta_1 = 10^{9.4}$ for $OH^-$ and $\beta_1 = 10^{5.45}$ for $Cl^-$ [15,33]) and should be compared to known affinities for chemical functions of phospholipid head-groups to predict reactivity. Unfortunately, no thermodynamic data for $CH_3Hg(II)$ complexation with phosphates was found in the literature. However, since the phosphate is the only potential mercury binding group in PA, we have to conclude that this affinity is quite strong. Lack of binding to the PC zwitterion conditions this complexation to the presence of a global negative charge on the membrane surface. This is confirmed by the intermediate binding curve obtained with mixed DMPA/DMPC. On the other hand, $CH_3Hg(II)$ shows a high affinity to primary amines ( $\beta_1 = 10^{7-8}$ [9]) and binds the serine amino-acid on the amine moiety [34]. Methylmercury

interactions with DMPE display distinct properties from binding to anionic lipids and the observed $^{31}$P-NMR line changes are very similar to those induced by Hg(II) binding to PE amino group [18]. It is therefore possible that $CH_3Hg(II)$ binds to the primary amine preferentially to the phosphate in zwitterionic PE. DMPE lower apparent affinity compared to anionic phospholipids could then be related to competition with $OH^-$ for $CH_3Hg(II)$ binding, due to close $\beta$ values. On the other hand, and because DMPA and DMPS show similar binding curves, methylmercury appears be a good candidate to bind to the phosphate group in anionic lipids. Since $CH_3Hg(II)$ affinity to carboxyls is only about $10^{2-3}$ [35], this rules out the carboxyl group as a potential binding site. However, the role of the amine in $CH_3Hg(II)$ binding by PS cannot be estimated from our results. Taken together, these results are indicative of electrostatic adsorption of $CH_3Hg^+$ at the negatively charged membrane surface, rather than specific $CH_3Hg(II)$-phosphate covalent binding.

Hg(II) and $CH_3Hg(II)$ therefore display very different specificities in their interactions with biological lipids. However, both share a strong affinity to a specific class of phospholipids and a tendency to accumulate into lipid bilayers, resulting in large structural effects (fluidity changes and integrity loss) that could induce severe functional perturbations at the biomembrane level. These molecular mechanisms play an essential part in their high neurotoxicity. It is often considered that by interacting with thiols and lipids Hg(II) promotes immediate damage to the cell while $CH_3Hg(II)$ crosses biomembranes easily and tends to accumulate into the cytosol, for later toxicological effects [5]. However, methylmercury also induces depolarization of nerve cell membranes, solubilization of red cell membrane proteins and membrane leakage at micromolar concentrations [12,36]. Binding to proteic thiols has been evoked to interpret these properties [1,37], but no mechanism was given to explain how formation of $CH_3Hg$-S-protein surface complexes could cause such extended membrane structural damage. Obviously, anionic phospholipids are major targets for methylmercury binding in biomembranes and the formation of non-bilayer lipid phases resulting from these interactions could be an important mechanism to account for $CH_3Hg(II)$ toxicity at the membrane level.

## 5. Conclusion

The use of three complementary physical techniques affords an overall view of the methylmercury-membrane interactions. Metal binding and its structural consequences on the bilayer fluidity and organization can thus be simultaneously detected, enabling to relate the observed macroscopic effects to specific molecular mechanisms. We demonstrated herein that strong metal binding (up to three $CH_3Hg(II)$ molecules per lipid) induces limited perturbations of membrane structure, though anionic phospholipids are obviously a major target for methylmercury complexation in biomembranes.

## References

[1] Rothstein, A. (1981) in The Function of Red Blood Cells: Erythrocyte Pathobiology, pp. 105–131, Alan R. Liss, New York.
[2] Major, M.A., Rosenblatt, D.H. and Bostian, K. (1991) Environ. Toxicol. Chem. 10, 5–8.
[3] Gutknecht, J. (1981) J. Membr. Biol. 61, 61–66.
[4] Bienvenue, E., Boudou, A., Desmazès, J.P., Gavach, C., Georgescauld, D., Sandeaux, J., Sandeaux, R. and Seta, P. (1984) Chem-Biol. Interactions 48, 91–101.
[5] Mason, R.P., Reinfelder, J.R. and Morel, F.M.M. (1995) Water, Air and Soil Pollut. 80, 915–921.
[6] Boudou, A., Delnomdedieu, M., Georgescauld, D., Ribeyre, F. and Saouter, E. (1991) Water Air Soil Pollut. 56, 807–821.
[7] Rouleau, C., Pelletier, E. and Tjalve, H. (1995) Mar. Ecol. Prog. Ser. 124, 134–158.
[8] Chen, R.W., Ganther, H.E. and Hoekstra, W.G. (1973) Biochem. Biophys. Res. Communicat. 51, 383–390.
[9] Rabenstein, D.L. and Fairhurst, M.T. (1975) J. Am. Chem. Soc. 97, 2086–2092.
[10] Takisawa, Y. (1979) in The biochemistry of mercury in the environment, pp. 500–502 (Nriagu, J.O. ed.), Elsevier, Amsterdam.
[11] Kinter, W.B. and Pritchard, J.B. (1977) in Handbook of Physiology (Section 9): Reactions to Environmental Agents, pp. 563–573, Williams and Wilkins, London.
[12] Nakada, S., Inoue, K., Nojima, S. and Imura, N. (1978) Chem-Biol. Interactions 22, 15–23.
[13] Segall, H.J. and Wood, J.M. (1974) Nature 248, 456–458.
[14] Leblanc, R.M., Joly, L.P. and Paiement, J. (1984) Chem-Biol. Interactions 48, 237–241.
[15] Sudmeier, J.L., Birge, R.R. and Perkins, T.G. (1978) J. Magn. Res. 30, 491–496.
[16] Delnomdedieu, M., Boudou, A., Georgescauld, D. and Dufourc, E.J. (1992) Chem-Biol. Interact. 81, 243–269.

[17] Delnomdedieu, M., Boudou, A., Desmazès, J.P. and Georgescauld, D. (1989) Biochim. Biophys. Acta 986, 191–199.
[18] Girault, L., Lemaire, P., Boudou, A., Debouzy, J.C. and Dufourc, E.J. (1996) Eur. Biophys. J. 24, 413–421.
[19] Tocanne, J.F. and Teissié, J. (1990) Biochim. Biophys. Acta 1031, 111–142.
[20] Rance, M. and Byrd, R.A. (1983) J. Magn. Res. 52, 221–240.
[21] Dufourc, E.J., Mayer, C., Stohrer, J., Althoff, G. and Kothe, G. (1992) Biophys. J. 61, 42–57.
[22] Lakowicz, J.R., Prendergast, F.G. and Hogen, D. (1979) Biochemistry 18, 508–519.
[23] Marsh, D. (1990) in Handbook of Lipid Bilayers, pp. 135–156, CRC Press, Boca Raton.
[24] Petersheim, M. and Sun, J. (1989) Biophys. J. 55, 631–636.
[25] Verkleij, A.J., De Kruyff, B., Ververgaert, P.H.J.T., Tocanne, J.F. and Van Deenen, L.L.M. (1974) Biochim. Biophys. Acta 339, 432–437.
[26] Delnomdedieu, M., Boudou, A., Georgescauld, D. and Dufourc, E.J. (1990) Bull. Magn. Reson. 11, 420 .
[27] Groombridge, C. (1993) Magn. Reson. in Chem. 31, 380–387.
[28] Boudou, A., Desmazès, J.P. and Georgescauld, D. (1982) Ecotoxicol. Environ. Safety 6, 379–387.
[29] Lakowicz, J.R. and Anderson, C.J. (1980) Chem-Biol. Interactions 30, 309–323.
[30] Ohki, S. and Ohshima H. (1984) Biochim. Biophys. Acta 776, 177–182.
[31] Seelig, J. (1978) Biochim. Biophys. Acta 515, 105–140.
[32] Rajan, S., Kang, S.Y., Gutowsky, H.S. and Oldfield, E. (1981) J. Biol. Chem. 256, 1160–1166.
[33] Smith, R.M. and Martell, A.E. (1976) Critical stability constants. Volume 4: Inorganic complexes. Plenum Press, New York.
[34] Corbeil, M.C. and Beauchamp, A.L. (1988) Can. J. Chem. 66, 1379–1381.
[35] Alex, S. and Savoie, R. (1987) Can. J. Chem. 65, 491–496.
[36] Shrivastav, B.B., Brodwick, M.S. and Narahashi, T. (1976) Life Sci. 18, 1077–1082.
[37] Medeiros, D.M., Cadwell, L.L. and Preston, R.L. (1980) Bull. Environ. Contam. Toxicol. 24, 97–101.
[38] Stary, J. and Kratzer, K. (1989) Toxicol. Environ. Chem. 22, 197–202.
[39] Pelletier, E. (1995) in Metal Speciation and Bioavailability In Aquatic Systems (Tessier A. and Turner D.R. eds.), Wiley, Chichester, pp. 103–148.
[40] Pott, T., Maillet, J.C. and Dufourc E.J. (1995) Biophys. J. 69, 1897–1908.